metals

MDPI

Article

The Effects of Homogenizing and Quenching and Tempering Treatments on Crack Healing

Yao Qiu [1,2], Ruishan Xin [3,4], Jianbin Luo [1,2] and Qingxian Ma [1,2,*]

1 Department of Mechanical Engineering, Tsinghua University, Beijing 100084, China; qiuy15@mails.tsinghua.edu.cn (Y.Q.); ljblqw@mail.tsinghua.edu.cn (J.L.)
2 Key Laboratory for Advanced Materials Processing Technology of Ministry of Education, Tsinghua University, Beijing 100084, China
3 Ansteel Beijing Research Institute, Beijing 102211, China; ruishanxin@163.com
4 HBIS Group Technology Research Institute, Shijiazhuang 050023, China
* Correspondence: maqxdme@mail.tsinghua.edu.cn; Tel.: +86-010-6277-1476

Received: 29 February 2020; Accepted: 24 March 2020; Published: 25 March 2020

Abstract: After thermal deformation and heat treatment, it can be observed that there are small, newly formed grains in the crack healing zone, which indicates that the internal crack is fully healed. However, in our previous study, the impact properties of the internal healing zone could only be partially healed. In this study, the process of homogenizing treatment was adopted to achieve grain size homogeneity. The effects of homogenizing treatment and quenching and tempering treatment on crack healing were also systematically analyzed. With the same heat treatment method, SA508-3 samples, which were subjected to multi-pass deformation, had a higher percentage recovery than those that underwent uniaxial compression. The percentage recovery of the crack healing zone was significantly improved after the process of homogenizing treatment. The impact property of the crack healing zone could be fully restored after homogenizing treatment followed by quenching and tempering treatment. However, after several episodes of heating, the grain-boundary strength decreased, and the impact value was relatively low.

Keywords: crack healing; impact property; homogenizing treatment; quenching and tempering treatment

1. Introduction

In the manufacturing process, it can be observed that internal defects appear inside large forgings such as porosities and internal cracks. In previous work, several methods were used for crack healing, including the isothermal heat treatment method [1–3], thermal deformation [4–7], and the electropulsing technique [8,9]. In the production of large forgings, the thermal deformation method followed by annealing is often used in internal crack healing. Han et al. [1,2] and Xin et al. [3] showed that after isothermal heat treatment at 1100 °C or a higher temperature, crack healing in steel could be achieved. Yu et al. [4] investigated the effects of different process parameters on crack healing and found out when the healing temperature, holding time, and reduction ratio increased, the recovery degree of the internal crack increased. Meng et al. [5] discovered that fine grains were formed in the process of crack healing. These grains firstly formed on the surface of the internal crack, and their morphology was different from that of the matrix. Xin et al. [6] and Qiu et al. [7] found that after annealing from the healing temperature, the tensile property could be fully restored, but the impact properties could only be partially restored, and this was related to the inhomogeneity of grain sizes.

Many researchers found that when internal defects were healed by a thermomechanical process, the resistance of steel against crack propagation also increased. Monhtadi et al. [10,11] investigated

the effect of cold rolling followed by annealing on the inhibition of hydrogen induced crack (HIC) initiation and propagation. The main reasons for increasing resistance included the formation of a desirable crystallographic texture and microstructure, low Kernel Average misorientation data, and coincident site lattice boundaries.

Previous studies mainly focused on the effects of process parameters, such as temperature, deformation rate, and cooling rate, on crack healing. The method of heat treatment used in the research was usually annealing. There has been little research on the effect of heat treatment methods on crack healing, especially homogenizing treatment and quenching and tempering treatment (Q & T).

The purpose of the present work was to study the effects of heat treatment methods on internal crack healing. The microstructure evolution and impact property of SA 508-3 samples with internal cracks were studied. Different heat treatments were compared with respect to their grain morphology and carbide distribution in the crack healing zone. Standard Charpy impact tests were carried out at room temperature to estimate the recovery degree of the impact property after different heat treatments.

2. Methods

SA 508-3 steel is a kind of low alloy steel, which is often used for the production of nuclear pressure vessels. The chemical composition of SA 508-3 steel is Fe-0.19C-0.22Si-1.4Mn-0.006P-0.006S-0.12Cr-0.53Mo-0.65Ni (wt%). Ingots of SA 508-3 steel (ϕ120 mm × 60 mm) were machined to prepare samples with preset internal cracks. The surface roughness of the cylinder was polished to 1.6 μm, and two cylinders were welded along the edges of contact surfaces. Thus, samples with internal cracks were prepared. An illustration of SA 508-3 sample preparation is shown in Figure 1.

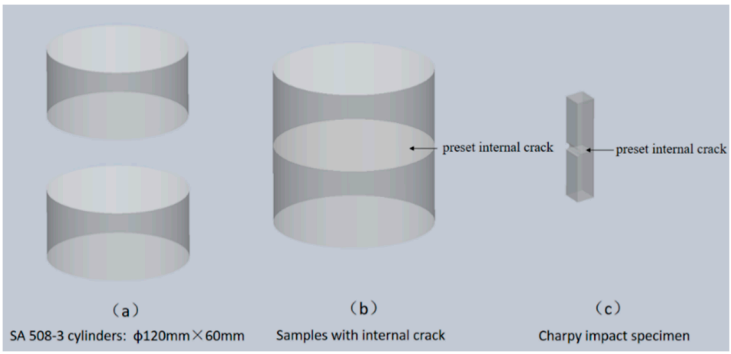

Figure 1. Illustration of SA 508-3 sample preparation. (**a**) SA 508-3 cylinders. (**b**) Sample with internal crack. (**c**) Charpy impact specimen.

In this study, the crack healing methods used were thermal deformation and heat treatment. The corresponding healing methods of samples are shown in Table 1.

The process of thermal deformation was conducted in an 8 MN forging machine. In the production of large forgings, the deformation process usually consists of several rounds of upsetting and stretching. In order to be more in accordance with actual production, the deformation processes used were uniaxial compression and multi-pass deformation.

Samples were heated to 1150 °C before thermal deformation. In uniaxial compression, the deformation rate was 20%, and the direction of compression was along the axis. The processing steps of multi-pass deformation were two rounds of upsetting and one round of stretching. The deformation rate of the first and second upsetting processes was 20%. In the process of stretching, the pressing order was 0° → 180° → 90° → 270° and the deformation rate of a single side was 20%. The process of multi-pass deformation is illustrated in Figure 2.

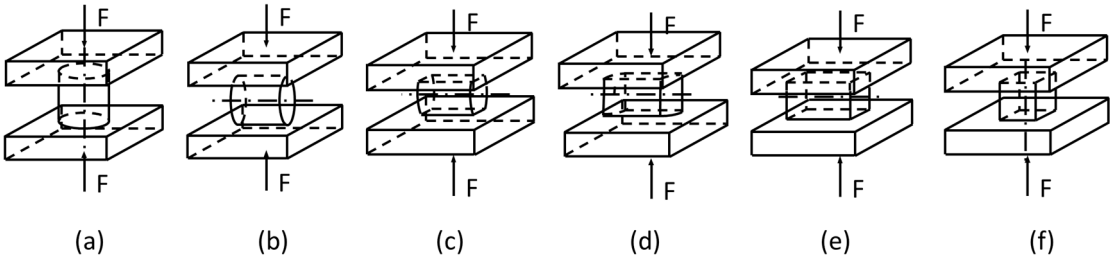

Figure 2. Schematic of the multi-pass deformation process. (**a**) the first upsetting (**b**–**e**) stretching (**f**) the second upsetting.

Nuclear pressure vessels have a vital role in the safe operation of nuclear power plants. Thus, this kind of large forging requires a high initial performance. To obtain good initial mechanical properties, quenching and tempering treatment is required in the production of SA508-3 steel [12].

The effects of homogenization heat treatment and tempering heat treatment on crack healing were studied. The parameters were set according to the actual production process. In the process of homogenization heat treatment, the samples were homogenized at 910 °C for 5 h before cooling in the air. In the quenching and tempering treatment, the samples were homogenized at 890 °C for 5 h followed by water quenching. Subsequently, the specimens were aged at 640 °C for 2 h and cooled in the air. Hereinafter, the samples healing by different methods are named as UC, UC-HT, UC-QT, UC-HT-QT, MD, MD-HT, MD-QT, MD-HT-QT, according to their healing methods. UC is short for uniaxial compression, MD is short for multi-pass deformation, HT is short for homogenization treatment, and QT is short for quenching and tempering treatment.

Table 1. The crack healing methods.

Sample	Deformation Modes	Heat Treatment	
		Homogenization Treatment	Quenching and Tempering Treatment
UC	Uniaxial compression	-	-
UC-HT	Uniaxial compression	homogenization treatment	-
UC-QT	Uniaxial compression	-	quenching and tempering treatment
UC-HT-QT	Uniaxial compression	homogenization treatment	quenching and tempering treatment
MD	Multi-pass deformation	-	
MD-HT	Multi-pass deformation	homogenization treatment	-
MD-QT	Multi-pass deformation	-	quenching and tempering treatment
MD-HT-QT	Multi-pass deformation	homogenization treatment	quenching and tempering treatment

To quantitatively describe the recovery degree of impact properties, the absorbed energy of the samples was measured at room temperature using Charpy impact tests on a 300 J pendulum impact test machine. Standard Charpy impact specimens with a U notch were machined both in the crack healing zone and in the matrix. In the specimens of the crack healing zone, the crack surface was set in the middle of the U notch, as shown in Figure 1c. The percentage recovery of the crack healing zone was obtained as the ratio of absorbed energy in the crack healing zone and the absorbed energy in the matrix.

To observe the morphology, the surfaces of samples were polished and etched by saturated picric acid. The microstructures of samples were observed with an optical microscope (OLYMPUS-CX41, Olympus, Tokyo, Japan) and a scanning electron microscope electron microscope (JSM-7100F, JEOL, Tokyo, Japan).

3. Results

3.1. Microstructure Evolution of the Crack Healing Zone

The morphology evolution could be observed using an optical microscope, as shown in Figure 3.

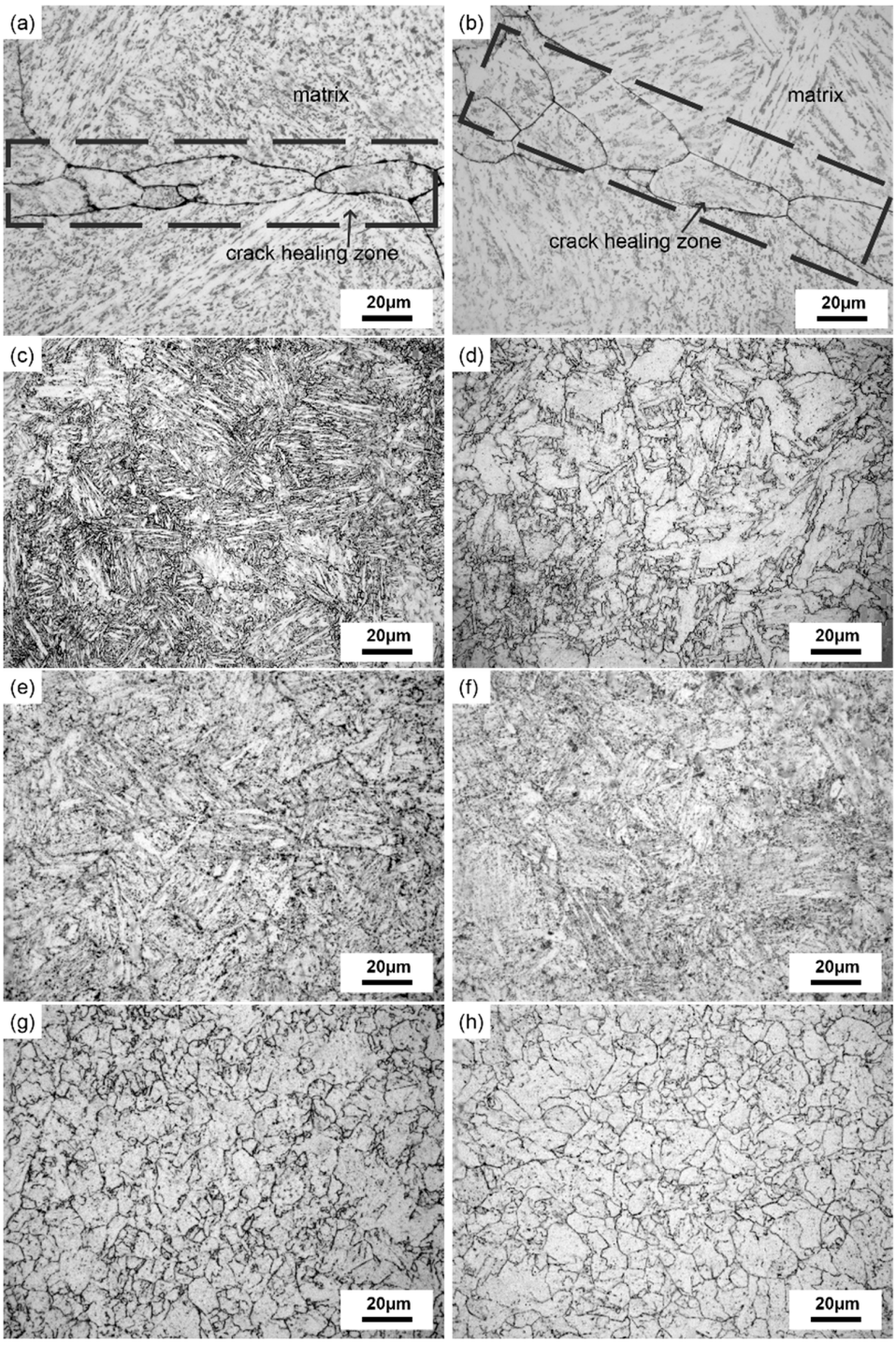

Figure 3. Microstructure evolution observed by an optical microscope. (**a**) UC, (**b**) MD, (**c**) UC-HT, (**d**) MD-HT (**e**) UC-QT, (**f**) MD-QT, (**g**) UC-HT-QT, (**h**) MD-HT-QT.

When the samples were cooling to room temperature in the air, newly formed grains appeared in the crack healing zones. The grain sizes in the crack healing zone were smaller than those in the matrix in samples UC and MD, as shown in Figure 3a,b. In our previous study [6], these small grains that appeared in the crack healing zones indicated that internal cracks were completely healed.

After homogenizing treatment, with the fast cooling rate, the microstructure evolved into lath bainite [12]. In sample UC-HT, the sizes of the laths inside the same grain were roughly the same, and they were arranged in parallel. In sample MD-HT, the spacing between laths was wider, and the

number of laths was fewer. It could be observed that grain homogenization was achieved in both the crack healing zone and the matrix in samples UC-HT and MD-HT, as shown in Figure 3c,d.

After quenching and tempering treatment without homogenizing treatment, the microstructure changed to tempered bainite, as shown in Figure 3e,f. However, when observed by an optical microscope, due to the low resolution, the morphologies of grains in the crack healing zone and the matrix were difficult to distinguish in samples UC-QT and MD-QT. Further observation was needed at a higher magnification.

When the samples underwent homogenizing heat treatment followed by quenching and tempering heat treatment, the grain size was significantly refined, and the grain sizes in the crack healing zones and the matrix were basically the same, as shown in Figure 3g,h. There was no significant difference in microstructure between the samples that underwent uniaxial compression and those that underwent multi-pass deformation.

3.2. Impact Property of Crack Healing Zone

The impact properties of samples healing with different healing methods are listed in Table 2. In order to quantitatively measure the degree of impact recovery, a Charpy impact specimen was also cut in the matrix. The percentage recovery of the impact property was measured as the ratio of absorbed energy in the crack healing zone to the energy absorbed in the matrix. The percentage recoveries after different heat treatments are shown in Figure 4.

Table 2. Impact property of SA 508-3 samples after different healing methods.

Healing Methods	Absorbed Energy in the Crack Healing Zone (J)	Standard Deviation (J)	Absorbed Energy in the Matrix (J)	Percentage Recovery (%)
UC	8.93	1.02	14.54	61.40%
UC-HT	31.36	2.11	33.34	94.06%
UC-QT	61.75	4.62	218.82	28.22%
UC-HT-QT	76.23	3.43	92.35	82.54%
MD	19.41	2.88	17.30	112.20%
MD-HT	33.45	5.12	33.98	98.44%
MD-QT	170.34	8.13	222.56	76.54%
MD-HT-QT	90.91	5.49	91.36	99.51%

each result is the average of three values.

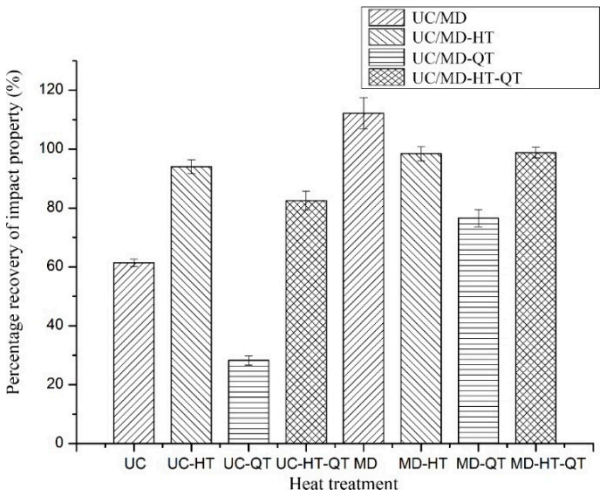

Figure 4. Percentage recovery of the impact property with different heating methods.

After the homogenizing treatment, the values of absorbed energy in the crack healing zone and the matrix increased. The percentage recovery of the impact property in the crack healing zone also significantly improved, when comparing samples UC and UC-HT.

After quenching and tempering heat treatment, the absorbed impact energy of the matrix and the crack healing zone significantly increased, but the recovery decreased percentage when comparing sample UC and UC-QT, MD and MD-QT.

When the samples underwent homogenizing heat treatment followed by quenching and tempering heat treatment, the impact properties acted as an intermediate state between only homogenizing heat treatment and only quenching and tempering heat treatment. When compared with UC-HT, the value of absorbed energy in the sample both in the crack healing zone and in the matrix of UC-HT-QT increased effectively. When compared with UC-QT, the recovery percentage of the impact property in UC-HT-QT significantly improved, but the absorbed impact energy reduced after several rounds of heating.

With the same heat treatment process, the samples healing by multi-pass deformation exhibited a higher impact property than the samples healing by uniaxial compression. Sample MD-HT-QT was able to achieve impact performance restoration.

A fractograph of different samples is presented in Figure 5.

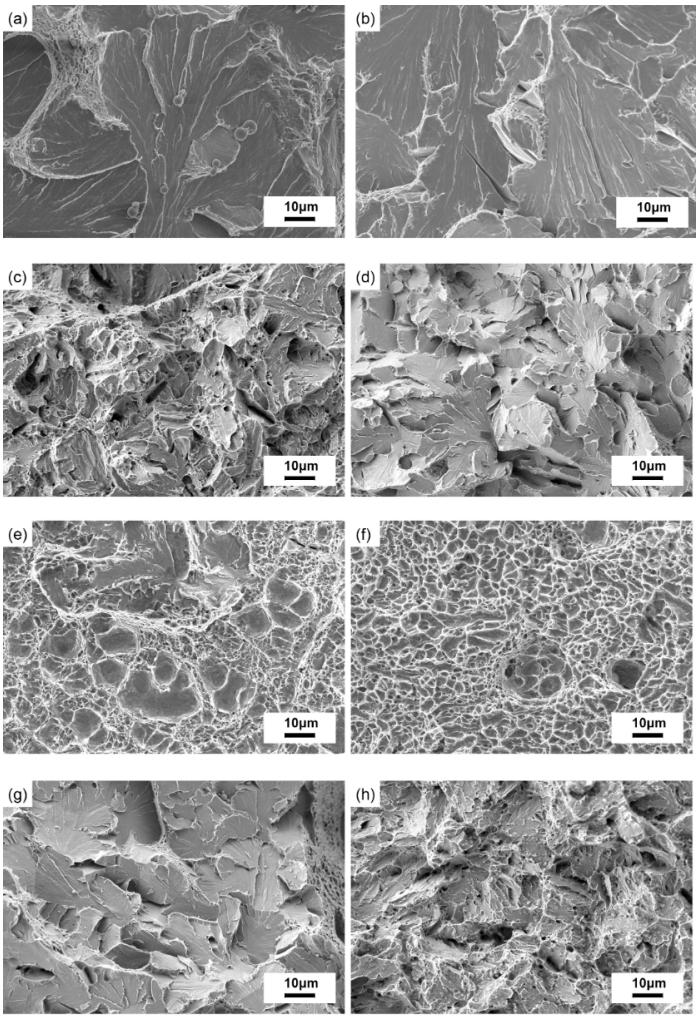

Figure 5. Fractograph of samples observed by scanning electron microscopy. (**a**) UC, (**b**) MD, (**c**) UC-HT, (**d**) MD-HT (**e**) UC-QT, (**f**) MD-QT, (**g**) UC-HT-QT, (**h**)MD-HT-QT.

When the samples were cooling in the air after thermal deformation, the impact fracture of the samples presented a river-like pattern in samples UC and MD, as shown in Figure 5a,b.

After the homogenizing treatment, a river shape pattern could still be seen in the fractograph, but the grain size was smaller in samples UC-HT and MD-HT, as shown in Figure 5c,d.

After quenching and tempering treatment, the fracture in sample UC-QT showed a complex morphology characterized by dimples and a cleavage fracture with a river pattern, as shown in Figure 5e. In sample MD-QT, the fracture morphology was mainly ductile micro dimples. The sizes of dimples were more even, and the average diameter was smaller than that of sample UC-QT.

After homogenizing heat treatment followed by quenching and tempering treatment, the impact fractograph mainly showed a river pattern, with small dimples along the grain boundary, as shown in Figure 5g,h.

4. Discussion

4.1. The Effect of Carbide Morphology on the Impact Property

From Figure 4, it is worth noting that after homogenizing treatment, the recovery percentage of the impact property significantly improved when comparing sample UC and sample UC-HT or sample UC-QT and UC-HT-QT.

The morphology of sample MD observed by scanning electron microscopy is shown in Figure 6. When the sample was cooling to room temperature in the air, the microstructure was granular bainite. In the crack healing zone, some voids could be observed, as shown in Figure 6a. The existence of voids could significantly reduce the impact property of the crack healing zone, resulting in incomplete recovery of impact property in sample MD.

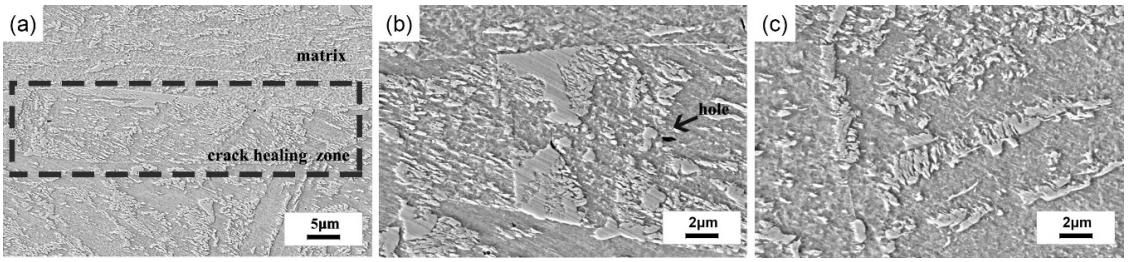

Figure 6. Morphology of sample MD observed by scanning electron microscopy. (**a**) MD, 2000×, (**b**) crack healing zone in sample MD, 5000× (**c**) matrix in sample MD, 5000×.

The morphology of sample MD-QT is shown in Figure 7. When the sample underwent quenching and tempering heat treatment, the microstructure was tempered bainite. It could be observed that both the grain sizes and carbide morphology in the crack healing zone were obviously different from those in the matrix. The carbides in the crack healing zone were mainly distributed along the grain boundary, and some small carbide precipitates inside the grain were elliptically shaped. In the matrix, the carbides were mainly observed inside the grain, presenting the characteristics of a lath-shaped morphology.

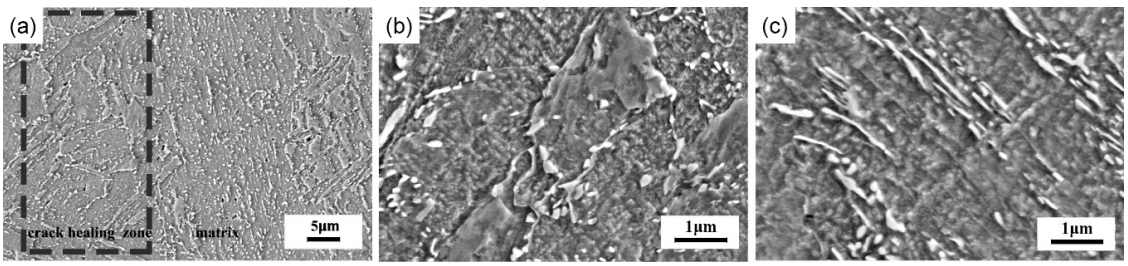

Figure 7. Morphology of sample MD-QT observed by scanning electron microscopy. (**a**) sample MD-QT, (**b**) crack healing zone in sample MD-QT, (**c**) matrix in sample MD-QT.

The reason for the grain size difference in sample MD-QT is related to the microstructure heredity. The SA 508 steel used in this study is a kind of low-carbon steel which has nonequilibrium bainite at room temperature. When heating to the critical temperature, thin lamellar austenite, which has a K-S orientation relationship with the parent phase would be formed at the lath boundaries. When the temperature continued to rise, lamellar austenite with the same position direction was easier to merge and grow; thus, large austenite grains formed, and microstructure heredity appeared [13]. In sample MD, there was a great difference in grain size between the crack healing zone and the matrix. The heating temperature in the quenching and processing treatment was 890 °C, and it was hard to get rid of microstructure heredity according to practical production experience. Thus, after the process of quenching and tempering, the grains in the matrix were coarser than those in the crack healing zone, and a grain size difference existed.

The difference in carbide morphology was affected by grain size. The tempering process of steel could be considered as the process of solid phase transformation controlled by the diffusion of C [14]. Johnson and Mehl [15], and Avrami [16–18] first proposed a relation to describe transformation controlled by diffusion. Watté et al. proposed a tempering kinetic law in the form of a J-M-A type equation, as follows [19]:

$$\tau = 1 - \exp(-DT^n). \quad (1)$$

τ is the tempering ratio, T is the tempering time, n is the Avrami exponent depending on the material, and D depends on the tempering temperature. The Arrhenius equation is as follows:

$$D = D_0 \exp\left(-\frac{Q}{RT}\right). \quad (2)$$

D_0 is the pre-exponential constant, Q is the activation energy of the tempering transformation, R is the perfect gas constant, and T is the tempering isothermal temperature.

In the same sample, the Avrami exponent n and tempering temperature T were the same in the crack healing zone and the matrix. The activation energy of the tempering transformation in bainitic steel was related to the grain size. The bigger the grain size was, the smaller the activation energy Q was [20]. The grain size of the matrix was bigger, the value of activation energy Q was smaller, and as shown by Equation (1) and Equation (2), the tempering ratio τ was higher in the matrix. Thus, after quenching & tempering treatment, in sample MD-QT, the size of precipitated carbides in the matrix was greater than those in the crack healing zone.

Previous researchers have found that the size of carbides could have a significant influence on the impact property. In tempered martensitic/bainite steel, it was illustrated that carbides or cracks formed by carbides are initiation sites for the fracture process [21,22]. Yan et al. [23] proposed that, in SA 508 steel, the existence of carbides could decrease the critical cleavage stress required for the initiation of microcracks, thus deteriorating the impact property. In our previous research [24], it was observed that cracks were deflected when they extended to the carbides. The crack propagation near the fracture surface in sample MD-QT is shown in Figure 8.

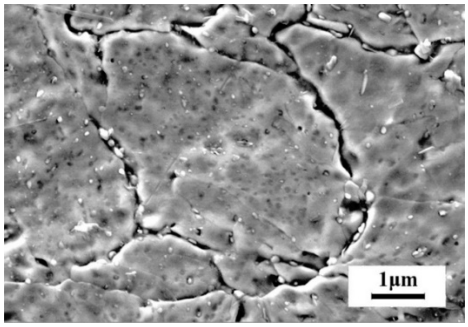

Figure 8. Crack propagation near the fracture surface in sample MD-QT.

The evolution mechanism can be explained as follows. When the tip of crack propagation was first encountered at the carbides, the crack was deflected and it spread along the carbide edge (Figure 9a,b) due to the change in stress distribution.

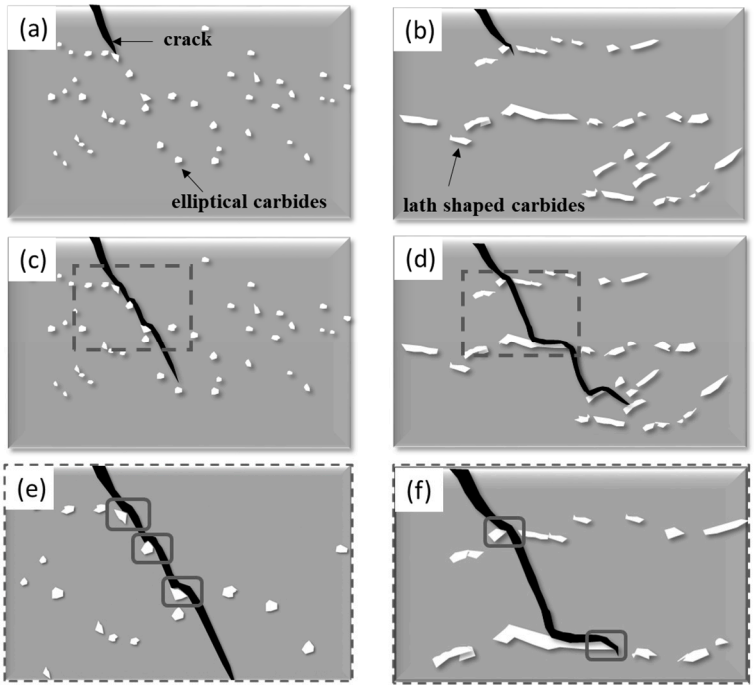

Figure 9. Crack propagation deflected by carbides.(**a**,**c**,**e**), elliptical carbides (**b**,**d**,**f**), and lath-shaped carbides.

When the crack came into contact with carbides, the degree of deflection in crack propagation due to lath-shaped carbides was higher than in elliptical carbides. The mechanism of action of the cracks and different morphologies of the carbides are shown in Figure 9e,f.

4.2. The Effect of Heat Treatment Methods on the Impact Property

The samples healed by different heat treatment methods are shown in Figure 10.

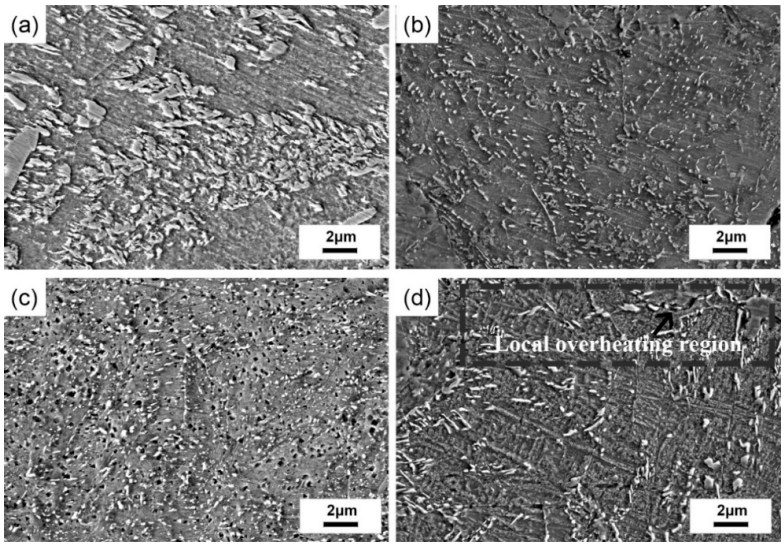

Figure 10. Morphologies of carbides after different heat treatments observed by scanning electron microscopy. (**a**) MD (**b**) MD-HT (**c**) MD-QT (**d**) MD-HT-QT.

After homogenizing treatment, there was no significant difference in grain size between the crack healing zone and the matrix. Uniformity of grain size was achieved in different regions of sample MD-HT and MD-HT-QT. To study the influence of heat treatment on the microstructure characteristics, the matrices of samples MD and MD-QT were used for comparison.

The homogeneity in carbide distribution between the crack healing zone and the matrix could be affected by the homogeneity of grain sizes. Thus, the percentage of the impact property in MD-HT and MD-HT-QT increased compared with that in samples MD and MD-QT.

After homogenizing heat treatment followed by quenching and tempering heat treatment, the precipitated carbides in sample MD-HT-QT were lath shaped and larger in size when compared with the small elliptic carbides in sample MD-QT.

When compared with sample MD-HT, the carbide content inside the grains of sample MD-HT-QT increased, as shown in Figure 10d. After tempering, carbide dispersed inside grains was able to enhance the strength inside SA508-3. Due to the effect of carbide morphology on the impact properties, the absorbed energy in sample MD-HT-QT was higher than that in sample MD-HT. However, after several heating processes, it could also be observed that local overheating occurred in some regions of sample MD-HT-QT. In the overheating region, microcracks occurred at the grain boundary, which could lead to the degradation of absorbed energy compared with sample MD-QT.

5. Conclusions

In summary, the effects of homogenizing treatment and quenching and tempering treatment were investigated with respect to the impact property recovery of crack healing in SA508-3 steel and its microstructure. The main results are summarized as follows:

(1) The samples healing by multi-pass deformation exhibited higher performance in the impact property than the samples healing by uniaxial compression with the same heat treatment process.

(2) The microstructure of tempered SA508-3 steels is tempered bainite with carbides precipitated in the grains and along the grain boundary. The quenching and tempering process will result in a reduction in the recovery percentage of the impact property due to the different morphologies of precipitated carbides in the matrix and the crack healing zone.

(3) The percentage recovery rate of the crack healing zone significantly improved after the homogenizing treatment process. The impact property of the crack healing zone could be fully restored after the combination of homogenizing treatment followed by quenching and tempering treatment. However, after several rounds of heating, the grain-boundary strength decreased, and the impact value was relatively low.

Author Contributions: Conceptualization, Y.Q., R.X. and Q.M.; methodology, Y.Q.; investigation, Y.Q. and R.X.; data curation, J.L.; writing—original draft preparation, Y.Q.; writing—review and editing, Y.Q. and R.X.; supervision, Q.M.; project administration, Q.M.; funding acquisition, Q.M. All authors have read and agreed to the published version of the manuscript.

Funding: This research and APC were funded by National Natural Foundation of China, grant number 51775298 and Hebei Natural Science Foundation, grant number E2019318022.

Acknowledgments: The authors gratefully acknowledge the financial support received from the National Natural Foundation of China (No. 51775298) and Hebei Natural Science Foundation-Iron and Steel Joint Funds (No. E2019318022).

Conflicts of Interest: The authors declare no conflict of interest. The supporting source had no such involvement.

References

1. Zhang, Y.J.; Han, J.T. Analysis of microstructure of steel 20 in the range of healing of internal crack. *Met. Sci. Heat Treat.* **2012**, *58*, 526–528. [CrossRef]
2. Wei, D.; Han, J.; Jiang, Z.Y.; Lu, C.; Tieu, A.K. A study on crack healing in 1045 steel. *J. Mater. Process. Technol.* **2006**, *177*, 233–237. [CrossRef]

3. Xin, R.S.; Ma, Q.X.; Li, W.Q. Effect of Heat Treatment on Microstructure and Hardness of Internal Crack Healing in a Low Carbon Steel. *Key Eng. Mater.* **2017**, *730*, 3–7. [CrossRef]
4. Yu, H.; Liu, X.; Li, X.; Godbole, A. Crack Healing in a Low-Carbon Steel under Hot Plastic Deformation. *Metall. Mater. Trans. A* **2014**, *45*, 1001–1009. [CrossRef]
5. Meng, F.Y.; Nie, S.M. Inner Surface Migration during the Internal Crack Healing in 45 Steel. In *Materials Science Forum*; Trans Tech Publications Ltd.: Dalian, China, 2009; Volume 628, p. 547. [CrossRef]
6. Xin, R.; Ma, Q.; Guo, D.; Li, W. Restoration of impact properties of internal crack healing in a low carbon steel. *Mater. Sci. Eng. A* **2017**, *682*, 433–440. [CrossRef]
7. Qiu, Y.; Xin, R.; Luo, J.; Ma, Q. Crack Healing and Mechanical Properties Recovery in SA 508–3 Steel. *Material* **2019**, *12*, 890. [CrossRef]
8. Hosoi, A.; Nagahama, T.; Ju, Y. Fatigue crack healing by a controlled high density electric current Field. *Mater. Sci. Eng. A* **2012**, *533*, 38–42. [CrossRef]
9. Zhou, Y.; Guo, J.; Gao, M.; He, G. Crack healing in a steel by using electropulsing technique. *Mater. Lett.* **2004**, *58*, 1732–1736. [CrossRef]
10. Mohtadi-Bonab, M.A.; Eskandari, M.; Szpunar, J.A. Role of cold rolled followed by annealing on improvement of hydrogen induced cracking resistance in pipeline steel. *Eng. Fail. Anal.* **2018**, *91*, 172–181. [CrossRef]
11. Mohtadi-Bonab, M.A.; Ghesmati-Kucheki, H. Important factors on the failure of pipeline steels with focus on hydrogen induced cracks and improvement of their resistance. *Met. Mater. Int.* **2019**, *25*, 1109–1134. [CrossRef]
12. Yan, G.; Han, L.; Li, C.; Luo, X.; Gu, J. Effect of macrosegregation on the microstructure and mechanical properties of a pressure-vessel steel. *Metall. Mater. Trans. A* **2017**, *48*, 3470–3481. [CrossRef]
13. Liu, N.; Liu, Z.; He, X. Structure Inheritance Removing of SA508 Gr. 4n Steel for Nuclear Reactor Pressure Vessels. *J. Iron Steel Res.* **2017**, *29*, 402–410. [CrossRef]
14. Zhou, Q.; Wu, X.; Shi, N. Microstructure evolution and kinetic analysis of DM hot-work die steels during tempering. *Mater. Sci. Eng. A* **2011**, *528*, 5696–5700. [CrossRef]
15. Johnson, W.A.; Mehl, R.F. Reaction kinetics in processes of nucleation and growth. *Trans. Metall. Soc.* **1939**, *135*, 416–442.
16. Avrami, M. Kinetics of phase change. I General theory. *J. Chem. Phys.* **1939**, *7*, 1103–1112. [CrossRef]
17. Avrami, M. Kinetics of phase change. II transformation-time relations for random distribution of nuclei. *J. Chem. Phys.* **1940**, *8*, 212–224. [CrossRef]
18. Avrami, M. Granulation, phase change, and microstructure kinetics of phase change. III. *J. Chem. Phys.* **1941**, *9*, 177–184. [CrossRef]
19. Watté, P. Strain aging in heavily drawn eutectoid steel wires. *Scr. Mater.* **1996**, *34*, 89–95. [CrossRef]
20. Li, X.; Zheng, Y.; Wu, X. Influence of Grain Size on Continuous Cooling Transformation Rules of a Bainitic Steel SDP1. *Mater. Rep.* **2017**, *31*, 86–92. [CrossRef]
21. Takebayashi, S.; Ushioda, K.; Yoshinaga, N.; Ogata, S. Effect of Carbide Size Distribution on the Impact Toughness of Tempered Martensitic Steels with Two Different Prior Austenite Grain Sizes Evaluated by Instrumented Charpy Test. *Mater. Trans.* **2013**, *54*, 1110–1119. [CrossRef]
22. Horn, R.M.; Ritchie, R. Mechanisms of Tempered Martensite Embrittlement in Low Alloy Steels. *Metall. Trans. A* **1978**, *9*, 1039–1053. [CrossRef]
23. Yan, G.; Han, L.; Li, C.; Luo, X.; Gu, J. Characteristic of retained austenite decomposition during tempering and its effect on impact toughness in SA508 Gr. 3 steel. *J. Nucl. Mater.* **2017**, *483*, 167–175. [CrossRef]
24. Qiu, Y.; Xin, R.; Luo, J.; Ma, Q. Effect of deformation modes and heat treatment on microstructure and impact property restoration of internal crack healing in SA 508-3 steel. *Mater. Sci. Eng. A* **2020**, *778*, 139073. [CrossRef]